Frequency scanning filtered Rayleigh scattering in combustion experiments

Ulrich Doll*, Michael Fischer, Guido Stockhausen, Christian E. Willert

Institute of Propulsion Technology, German Aerospace Center (DLR), 51147 Cologne, Germany
* Correspondent author: ulrich.doll@dlr.de

Abstract To increase the overall efficiency in aero engines as well as stationary gas turbines detailed information on flow field properties under realistic operating conditions are required. While conventional probe based technology is readily available and thoroughly tested, most of these techniques are point-wise. To gain insight into complex flow structures spatially and temporally resolved data is needed. Planar optical measurement techniques are capable of providing this type of data in a cost effective manner. The paper describes an image based filtered Rayleigh scattering (FRS) technique that, on frequency scanning a narrow linewidth light source, provides time averaged temperature (or density) fields. FRS uses molecular absorption to attenuate elastically scattered light from surfaces or particles in the flow. The filtered light is collected by a camera sensor at a multitude of light source frequencies allowing the temperature to be inferred from the pixel intensities. The measurement technique is validated on a McKenna type premixed flame and shows a better than 2% agreement to corresponding single point CARS measurements. The technique is further applied on a pressurized single sector combustor in an effort to visualize and quantify the cooling film on an effusion cooled combustor liner wall. In this case the light sheet was directed straight onto the wall and aligned with a single row of effusion holes. Due to the molecular filtering the laser flare on the wall was completely attenuated in the acquired images allowing temperature measurements to within a tenth of a millimeter from the liner wall.

1. Introduction

To increase the overall efficiency in aero engines as well as stationary gas turbines detailed information on flow field properties under realistic operating conditions are required. While conventional probe based technology is readily available and thoroughly tested, most of these techniques are point-wise. To gain insight into complex flow structures spatially and temporally resolved data is needed. Planar optical measurement techniques are capable of providing this type of data in a cost effective manner.

In an on-going effort to qualify optical measurement techniques for applications in machine-oriented test rig environments a modified filtered Rayleigh scattering (FRS) technique based on frequency scanning [Forkey1996a] was developed and is the main subject of this contribution. FRS makes use of the absorption bands of atomic or molecular gases to remove strong elastic scattering effects from the measured signal from, such as scattering from surfaces or scattering from dust and soot particles. This makes FRS especially suitable to visualize flow properties in the vicinity of walls [Brübach2006].

In combustion diagnostics, most Rayleigh scattering and FRS systems reported in the literature use narrow linewidth pulsed laser sources (100 – 150 MHz) [Most2001, Zetterberg2008] to illuminate the measurement plane, allowing short camera exposure times and thus reducing background contributions from flame luminosity or blackbody radiation. While being advantageous in this respect, an insufficient suppression of laser induced background noise in FRS measurements is reported by a number of researchers using pulsed laser sources. In [Forkey1996a], a Lorentzian broadening of the spectral lineshape of the laser is indicated and a direct measurement of the laser induced background level by evacuating the test cell is proposed. A residual longitudinal mode competition in the laser's oscillator is reported in [Kearney2005], resulting in a 5 – 10 % bias of the acquired signal.

The FRS implementation described in this paper follows a different approach by focusing on time-

averaged measurement rather than providing instantaneous results. The FRS system is based on a continuous wave (cw) diode-pumped solid state frequency-doubled Nd:YVO_4 laser and a molecular iodine absorption filter. The laser provides single frequency light at 532 nm with a spectral linewidth less than 5 MHz. No background light induced by laser line broadening was observed using this light source.
In frequency scanning FRS (fs-FRS) the laser's frequency is tuned along the absorption profile of the iodine filter providing an n-tuple of grayscale intensities for each camera pixel, with n as the number of scanning frequencies. In contrast to the fs-FRS system presented in [Boguzko2005], the scanning range is limited to frequencies were the optical density of the iodine absorption filter is sufficient to completely suppress the elastically scattered background light. Thus, provided that the gas composition, the pressure and the velocity are known, the measured intensity of every camera pixel for every frequency step is only a function of gas temperature.
In order to qualify fs-FRS for temperature measurements in combustion environments, time-averaged temperature distributions in atmospheric laminar lean premixed CH_4/Air flames were obtained and compared to single point temperature measurement provided by coherent anti-Stokes Raman scattering (CARS). In a second application fs-FRS is used to resolve the near-wall temperature distribution of the flame wall cooling film interaction in a pressurized generic single sector combustor at 5 bar.

2. Theoretical Background

2.1 Motivation of molecular filtering

Rayleigh scattering makes use of the fact that elastically scattered laser light from atoms and molecules, holds information on density, pressure, temperature and velocity inside the observed region of interest. Point wise, spectrally resolved Rayleigh scattering has been applied in multiple flow property measurements with sampling rates up to 10 kHz [Mielke2009]. In combustion experiments, Rayleigh scattering thermometry has been used as a temperature standard to calibrate a laminar premixed propane/air flame with an uncertainty of less than 1 % [Sutton2006].
Rayleigh scattering is several orders of magnitude weaker than other elastic scattering effects such as geometric scattering from surfaces and windows or Mie scattering from larger particles such as dust or soot. Because of this the accuracy of Rayleigh scattering measurements strongly depends on proper treatment of background noise effects and stray light suppression. The complexity of accurately determining the undesired but nonetheless omnipresent background signal becomes increasingly challenging when extending the technique to planar measurements. The avoidance of strong reflections from surfaces or windows is the first measure of choice. The suppression of the contribution of large particles to the measured signal can be achieved by actually (mechanically) filtering the particles from the examined flow [Panda2004]. In [Fourguette1986] it is proposed to measure the background level by flooding the test section with helium, which has a Rayleigh scattering cross section of about 75 times less than e.g. nitrogen or oxygen. Since these methods require extensive procedures and are at best suitable under laboratory conditions, the alternative of filtered Rayleigh scattering [Miles1990] seems to be best suited for providing a Rayleigh signal without the presence of the strong elastic scattering from larger particles (Mie scattering) or surfaces. In FRS the suppression is achieved with the absorption bands of atomic or molecular gases, which filter strong elastic scattering components from the measured signal.
To demonstrate the efficiency of molecular filtering, a simple experiment was performed [Zetterberg2008]: As illustrated in Fig. 1, a laser beam was formed into a light sheet and directed onto a metal plate. The bright primary reflex of the impinging laser light as well as scattering from dust particles inside the light sheet and a diffuse illuminated background can bee seen. The detector

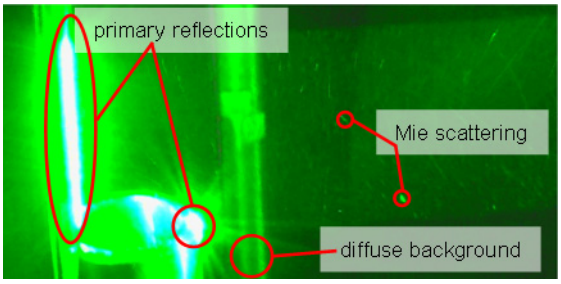

Fig. 1: Photograph of a light sheet directly impinging onto a metal plate. The bright primary reflex of the impinging light sheet, scattering from particles inside the light sheet and a diffuse illuminated background are visible.

was located perpendicular to the plane of the light sheet, observing both the primary reflex and a part of the light sheet through a band pass filter and a molecular absorption cell. The left hand side of Fig. 2 shows an image taken with an exposure time of 30 ms with the laser's frequency tuned out of the absorption band of the molecular filter. The strong primary reflection of the light sheet impinging the metal as well as the diffuse illuminated background are clearly visible. In the region of the primary reflex, the detector's pixel elements are saturated, resulting in characteristic blooming. On the right hand side of Fig. 2, the laser's frequency was tuned to the minimal transmission through the molecular filter. The camera exposure was 240 s. The strong elastic stray light of the primary reflex and the background are absorbed by the molecular filter. Instead, the light scattered off the air molecules, the Rayleigh scattering, illuminated by the laser light sheet becomes visible.

Fig. 2: Images acquired of a laser light sheet impinging onto a metal plate. With the laser tuned to the transmission minimum of the absorption cell the laser flare on the surface is essentially eliminated (camera exposure times: left, 30 ms; right, 240 s)

2.2 Working principle and extension to frequency scanning FRS

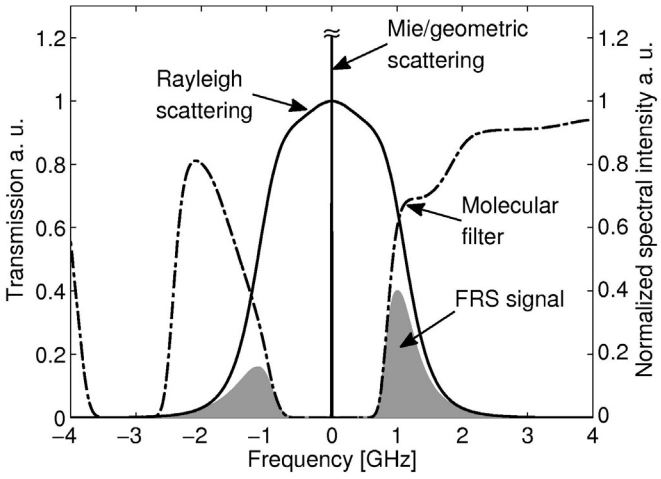

Fig. 3: FRS working principle: the narrow bandwidth light scattered from large particles (Mie) or surfaces (geometric) is absorbed by the iodine filter, while parts of the Rayleigh scattering pass through.

In FRS the filtering is achieved with the absorption bands of atomic or molecular gases, which filter strong elastic scattering components from the measured signal. Fig. 3 illustrates the spectral response of a volume illuminated with a narrow linewidth light source. The scattering from particles in the Mie regime (0.1-1 µm diameter) and the light scattered from surfaces have the same narrow spectral bandwidth and frequency as the illuminating light source. In contrast to this the Rayleigh scattering intensity profile has a spectral bandwidth of several gigahertz based on broadening mechanisms related to the molecular motion [Miles2001]. By placing the iodine filter in front of the detector, the filter's transmission curve is superimposed on the spectral signal response of the observed

volume element. Spectral shares inside the blocking range are absorbed by the filter, including the Mie and geometric scattering, but also a considerable amount of the Rayleigh scattered light is attenuated. The remaining spectral contributions of the Rayleigh signal that pass the filter can be accumulated by a sensitive detector and comprise the FRS signal from which further information such as temperature can be deduced.

The intensity collected by the detector can be described as the convolution of the total spectral intensity and the filter's transmission profile [Elliott1997]. To calculate the convolution, the Rayleigh scattering's spectral lineshape has to be determined. The S6 model introduced in [Tenti1974] is considered to be the most accurate model for diatomic molecules [Young1983], which is confirmed by recent measurements of the Rayleigh-Brillouin scattering lineshapes of several gas species as well as air [Vieitez2010]. The S6 model will be applied throughout this work. It describes the scattering regime by defining a dimensionless regime variable called y-parameter and a dimensionless frequency x:

$$y = \frac{p}{Ku_0\eta} = \frac{nk_BT}{\sqrt{2}Ku_0\eta}, \quad x = \frac{2\pi(\nu - \nu_0 - \Delta\nu)}{\sqrt{2}Ku_0}. \tag{1}$$

The y-parameter is a function of the pressure p (or the number density n through the ideal gas law), the temperature T, the norm of the scattering wave vector $K = 4\pi/\lambda_0 \sin(\Theta/2)$, the thermal velocity $u_0 = \sqrt{k_BT/m}$ and the shear viscosity η. θ is the angle between the propagation direction of the laser and the observer, m is the molecular mass of the scattering gas species and k_B is Boltzmann's constant. Δν is a Doppler shift arising from convective molecular motion. The resulting grayscale intensity for each camera pixel element is given by [Forkey1996a, Pitz1976]

$$S(x,y) = R(I_0)n\sum_k \chi_k\sigma_k\sigma_{FRS,k}(x,y) + B(I_0)\tau(\nu_0) + C. \tag{2}$$

The first term on the right hand side represents the FRS intensity. R, being proportional to the incident light's intensity I_0, describes the efficiency of the optical setup. To account for a measurement volume comprised of multiple gases, the total spectral intensity scattered can be described by the sum of the scattering intensities of the k gas species $\sigma_{FRS,k}$, weighted with the molefraction χ_k and the Rayleigh scattering cross section σ_k [Pitz1976]. $\sigma_{FRS,k}$ is calculated from the convolution of the transmission profile of the molecular filter τ and the Rayleigh scattering line profile r_k [Forkey1996a]

$$\sigma_{FRS,k}(x,y) = \int_{-\infty}^{\infty} r_k(x,y)\tau(\nu)d\nu\,. \tag{3}$$

The second term $B(I_0)\tau$ on the right hand side of equation (2) describes a residual background induced by the narrowband elastic scattering sources mentioned earlier. The product is a measure for the amount of light passing through the molecular filter, with B as a function of the incident light's intensity. The parameter C of the third term contains miscellaneous background sources, such as camera offset and flame luminosity. Throughout this work, all gas specific parameters will be assumed known and constant. For a closed solution of equation (2) both the model parameters R, B, C as well as the flow properties p, T, Δν have to be determined.

To interpret the measured grayscale intensity S(x,y) as temperature, one approach, followed by most research groups applying FRS to combustion [Elliott2001, Most2001, Kearney2005, Zetterberg2008], is to reduce the number of unknown parameters. Assuming that no narrowband laser induced stray light passes the filter and that no miscellaneous background sources are present or that they can be determined, only the first term on the right hand side of equation (2), representing the Rayleigh scattering, remains. Furthermore, if gas composition pressure and velocity are known, the parameter dependency is reduced to R and T. By normalizing the FRS signal with a measurement taken under reference conditions, the measured intensity is only a function of temperature.

A second approach is the frequency scanning method, first presented in [Forkey1996a]. In contrast to the above described strategy, the fs-FRS aims not on determining the unknown parameters of equation (2) from assumptions, but on extracting them out of measured data. As illustrated in Fig. 4 on the left hand side, the laser is tuned in frequency n-times along the molecular filter's absorption line. Acquiring images at discrete frequency steps results in intensity spectra for each camera pixel. By comparing the measured spectra to simulated data, in theory, the model parameters R, B, C as well as the flow field properties p, T, Δν can be determined.

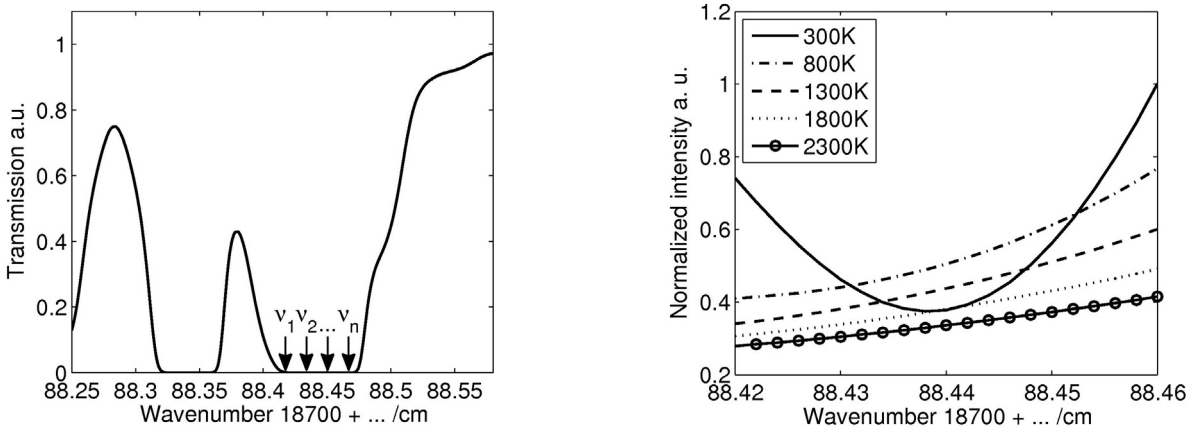

Fig. 4: (left) The laser's frequency ν is modulated n-times along the transmission curve (right) Simulated intensity profiles for air at 1 bar for varying temperatures

Comparing the two methods, the first approach offers the possibility to investigate instantaneous phenomena. A drawback of the first method lies in its ambiguity and in its susceptibility to noise. The right hand side of Fig. 4 shows FRS intensity spectra simulated for air at 1 bar over a wide temperature range. Especially at temperatures below 1500 K, intensity values at certain frequencies resemble two or more temperatures. Regarding temperatures above 1500 K, the sensitivity of the FRS intensity to temperature decreases. Particularly at frequencies, where the absorption of the molecular filter is highest, the measurement is the most susceptible to noise. In consequence, the frequency has to be carefully chosen regarding ambiguity, sufficient filtering and sensitivity.
While the frequency scanning method is suited for steady flows or time averaged measurements only, it does overcome most of the previously mentioned shortcomings. In measuring intensity profiles instead of single values, the correlation between temperature and intensity spectrum is distinct. The susceptibility to noise is reduced for the very same reason, offering the possibility to reduce the overall measurement uncertainty.
The present work will follow a combination of the two methods. In contrast to previous approaches [Forkey1996b, Boguszko2005], the scanning frequencies are limited to a region where the molecular filter is optically thick, so that all elastically scattered stray light is absorbed. In constraining the frequencies the scanning range is comparably small (~1 GHz to ~6 GHz in [Boguszko2005]), making the determination of a multitude of parameters difficult. Aiming on highly accurate temperature measurements, additionally, pressure is assumed known and velocity influence is assumed negligible. R and, if necessary, C are calculated from a reference frequency scan under known temperature conditions. Finally, the temperature is determined from a frequency scan under operating conditions.

3. Experimental apparatus

Fig. 5 gives an overview of the experimental apparatus and the optical arrangement. The FRS system is based on a Coherent Verdi continuous wave diode-pumped solid state frequency-doubled Nd: YVO_4 laser. The laser provides single frequency light at 532 nm with a spectral linewidth less

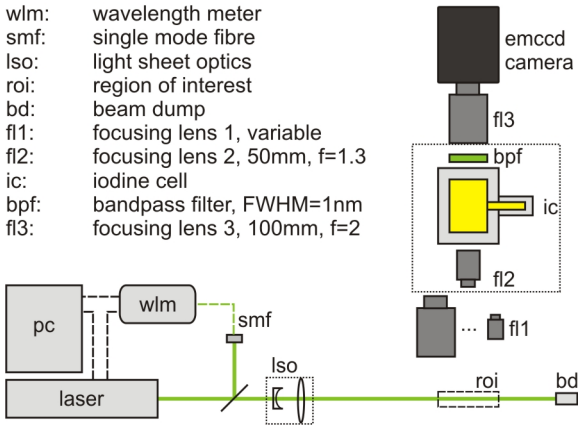

Fig. 5: Principal setup and optical arrangement of the FRS system

than 5 MHz and an adjustable output power of up to 5 W. The laser system features three options to alter its output frequency inside a tuning range of around 60 GHz. A heated etalon in the laser's cavity allows for large frequency modifications and two piezoelectric elements alter the resonator length. A small amount of laser light is coupled into a single mode fiber and connected to the frequency monitoring and controlling device, a High Finesse WSU 10 Wavelength meter. The device measures the laser's frequency with an absolute accuracy of 10 MHz. A built-in PID controller is connected to one of the laser's piezoelectric elements, stabilizing the output frequency with a relative accuracy less than 2 MHz. The long term stability of the laser's frequency is ensured by a second PID controller, issuing a control voltage onto the second piezoelectric input.

After being formed into a light sheet, the laser illuminates the interrogation area. For a maximum of Rayleigh scattering intensity, the detector is oriented perpendicular to propagation and polarization of the laser [Miles2001]. The scattered radiation is collected by a first focusing lens, which can be chosen variably with respect to the magnification needed. The collected light then enters the transfer optics, consisting of two focusing lenses in retro position. In between the two lenses, the molecular filter and a Barr bandpass filter with 1 nm FWHM and an optical density $>10^6$ out of passband are positioned. Finally the light is focused onto the camera chip of a back illuminated Hamamatsu C9100-13 EM-CCD camera. The camera has a maximum resolution of 512 x 512 pixel elements with a pixel size of 16 x 16 μm^2. Quantum efficiency is greater than 90 % for green light. Additionally, the camera features an amplification mechanism with an adjustable signal gain of up to 1200. The FRS camera system can be seen in Fig. 6 on the left hand side. It was designed for operation under test rig conditions, with the emphasis on flexibility and robustness.

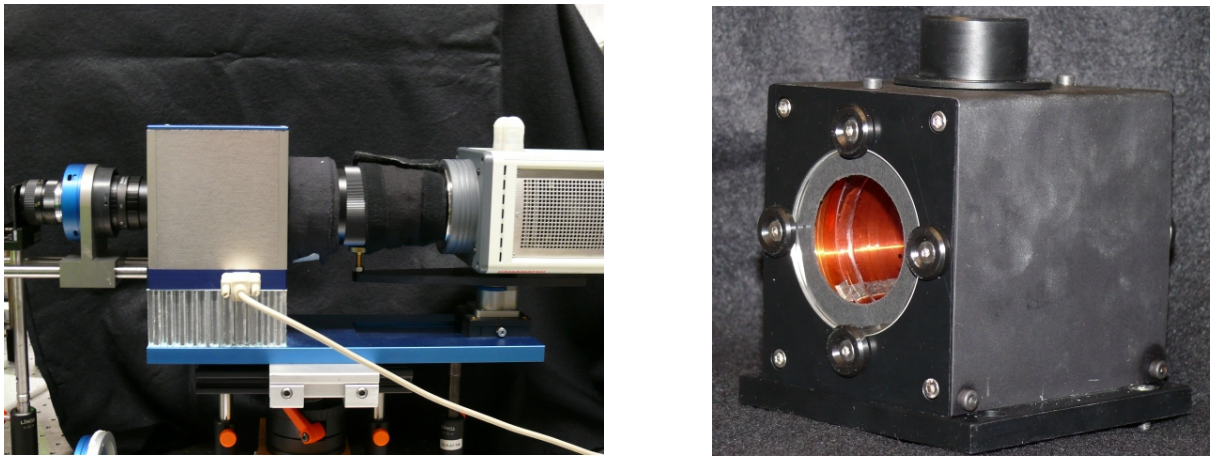

Fig. 6: The FRS camera system (left). The glass cylinder filled with molecular iodine inside a solid block of copper enclosed by a thermally insulating housing (right).

Molecular iodine was chosen for the absorption filter because of its numerous transitions in the vicinity of 532 nm. An image of the packaged iodine filter unit can be seen on the right hand side of Fig. 6. The filter consists of an evacuated glass cylinder, 50 mm in diameter and length, filled with a certain amount of crystalline iodine. The cylinder is mounted into a temperature controlled solid block of copper. When the cell is heated, the crystalline iodine begins to vaporize. Above a certain saturation temperature, all crystalline iodine is evaporated, leading to homogenous absorption

throughout the cell body on the one hand and preventing jumps in the filter's transmission by spontaneous evaporation of iodine on the other hand [Röhle2001]. The overall absorption of the filter, that is, it's optical density, is characterized by the vapor pressure of the iodine within the glass cylinder.
Concerning the McKenna burner experiment, a sufficient suppression of elastically scattered stray light over the whole frequency scanning range was achieved with an iodine filter cell saturating at a temperature of 70 °C. The near-wall measurements required a much stronger attenuation of elastic stray light due to strong reflections from walls and windows. An absorption filter with a saturation temperature of 80 °C was chosen for this application. Whereas the 80 °C filter unit has a minimum transmission of 10^{-32} compared to 10^{-19} of the iodine cell saturated at 70 °C (simulated values, [Forkey1996a]), more spectral shares contributing to the Rayleigh signal are blocked because of broader absorption lines and stronger continuum absorption using the 80 °C filter cell.
The entire experimental apparatus is embedded into National Instruments LabView routines and is controlled via a personal computer. This makes the system highly flexible concerning the integration of varying hardware components such as laser or camera system.

4. Application examples

4.1 Atmospheric combustion

The atmospheric CH_4/Air flame under investigation was provided by a flat-flame McKenna type matrix burner. Fuel and air are mixed inside a cavity below the burner plate before being released through a cooled bronze matrix. The exhaust gas behind the reaction zone is characterized by a temporally and spatially uniform temperature distribution and species concentration [Sutton2006].

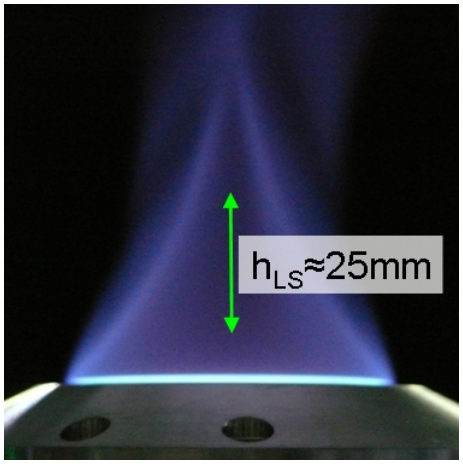

Fig. 7: Laminar flame of a McKenna type flat-flame burner of 60 mm diameter.

Fig. 7 shows a typical laminar diffusion flame of a McKenna flat-flame burner. A characteristic blue glowing cone of hot exhaust gas is present behind the reaction zone. The bright blue region right above the burner matrix coincides with the actual flame front. Due to the broadband luminosity of the flame front the interrogation window was chosen to begin ~14 mm above the burner plate and extended over ~25 mm in height.
The left hand side of Fig. 8 shows the result for a single pixel element (x = 0 mm, y = 15 mm) of a temperature analysis in a laminar lean premixed flame ($\Phi = 0.8$, $CH_4 = 1.31$ slpm, Air = 15.6 slpm) provided by the McKenna type flat field burner. The model equation is fitted to the measured data of the frequency scan in a least squares sense using a Levenberg-Marquardt algorithm [Vetterling1992]. This results in a temperature of 1733 K. The relative residual is a measure for the goodness of the fit and lies well below 1 %. The point-wise CARS result of 1765 K [Weigand et al.] corresponds to the FRS temperature within less than 2 %.
On the right of Fig. 8, the fitting algorithm was applied to each camera pixel, resulting in a temperature map of the burner flame. The temperature field shows an overall decrease of ~200 K from to lowest vertical position of 14 mm to the highest of 35.5 mm. Within the core region of the flame, the horizontal temperature distribution is nearly constant for each vertical position. At the edges of the cone, the temperature drops rapidly due to cold air mixing with the hot exhaust gas. In this region the measurement uncertainty rises, because the gas composition is no longer stable.

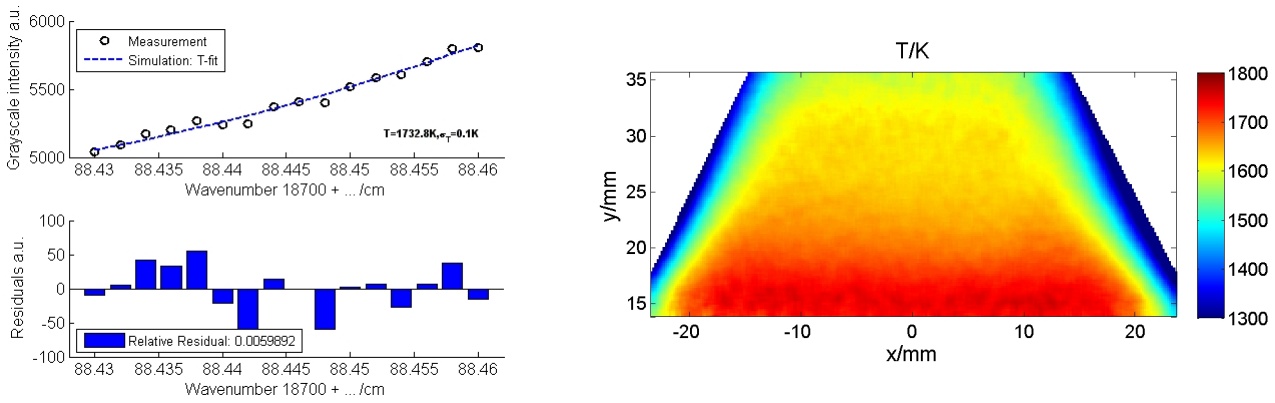

Fig. 8: Left: The temperature for a given pixel is determined by applying a nonlinear least squares fit of the model equation (blue dashed line) to the measured data (black circles). Right: The fitting routine is applied to each camera pixel resulting in a temperature map of the burner flame.

4.2 Near-wall measurements

Efficient cooling by a field of closely neighbouring film cooling holes is required to prevent thermal stress on the combustor liner walls, resulting from thermal patterns on the surface produced by the interaction of impinging combustor flame and cooling jets. Therefore the cooling efficiency plays an important role for the thermal stability of new wall materials needed for the increased working temperatures and pressures of gas turbine combustors which are necessary for increased turbine efficiencies. The analysis of the spatial effectiveness of the effusive film-cooling is of special importance due to reduced cooling air flows in modern lean combustor concepts [Gerendás2001] which results in an increased interaction between combustor flow and cooling film. The development of measurement techniques for the near-wall temperature field is aimed on the non-intrusive measurement of heat transfer between gas phase and cooled combustor wall. While the surface temperature is accessible by thermocouples (intrusive), thermographic phosphors [Brübach2006] or IR imaging [Behrendt2008] the near wall gas phase temperature is measurable pointwise by coherent anti-Stokes Raman scattering (CARS) or two dimensional by Filtered Rayleigh Scattering (FRS) [Elliott2001, Brübach2006].

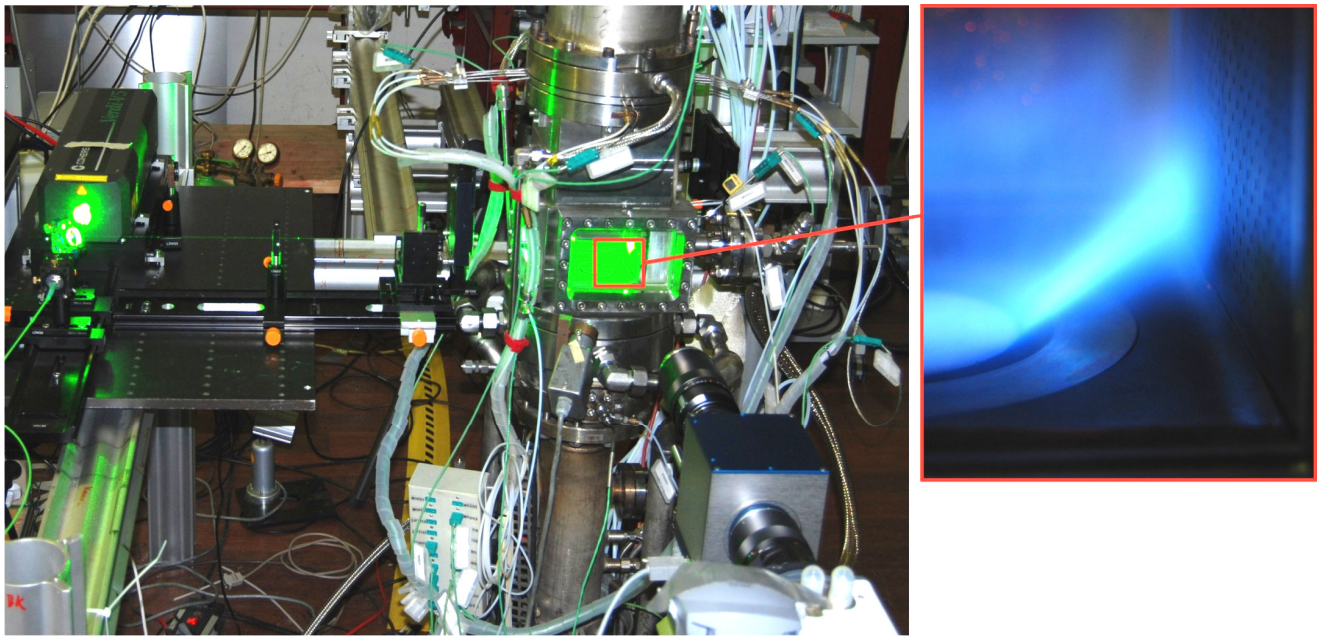

Fig. 9: FRS set-up on a generic combustor (left) and zoomed flame image with effusion cooled wall (right)

Within the context of optimizing effusion cooling concepts for liner walls, the fs-FRS technique was applied. Being independent of laser induced stray light off windows and walls, FRS was chosen to give a spatially resolved impression of the temperature distribution of the coolant film flame interaction in the direct vicinity of the liner wall.

The measurements were carried out on a high pressure single sector combustor (SSC) facility at DLR Cologne [Meier2011]. The SSC has a cross sectional area of 102 x 102 mm^2 and is capable of operation up to pressures of 20 bar at air preheating temperatures of up to 850 K. The maximum mass flows are 1 kg/s for primary air and 2 kg/s for cooling air. The test rig is optically accessible from three sides and traversable in three orthogonal directions. For the present investigations the SSC was operated with natural gas at a mass flow of 4.5 g/s and an air mass flow of 72.5 g/s (AFR ~17). The combustion chamber was pressurized at 5 bar, primary and cooling air were preheated to 450 K. The FRS images were obtained in the same measurement plane as the PLIF and PIV measurements presented in [Lange2012].

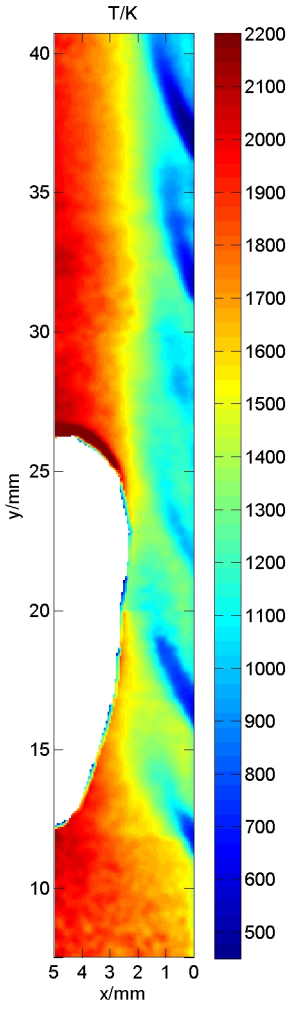

Fig. 10: Near-wall temperature field generated from FRS data at 5 bar and 450 K cooling air temperature.

An image of the optical setup and the test rig is shown in Fig. 9 on the left. The light exiting the laser was deflected by 90 ° and formed into a sheet. The light sheet was positioned normal to the effusive cooling plate (Fig. 9, right) and aligned with the central row of air jets (hole diameter 0.6 mm). The detector was placed perpendicular to the plane containing the laser. In order to visualize the interaction between coolant jet and flame in detail, the field of view was limited to 16 x16 mm^2 covering two effusion air jets, with the lower edge of the first jet at 11 mm above the burner plate. By traversing the combustor in two increments of 10 mm vertically, it was possible to examine six coolant jets. At this magnification a sensor pixel corresponds to 0.0625 mm in object space. The camera lens was a Zeiss MacroPlanar f = 100 mm, F = 2 with a working distance (camera lens – laser light sheet) of 340 mm. The light sheet's thickness was about 0.4 mm, the height 11 mm. During the frequency scan light was accumulated for 4 s at 20 different laser frequencies.

Fig. 10 shows the first 5 mm of the near-wall temperature distribution combined from the three measurements corresponding to the three vertical combustor positions. Doppler shifts arising from convective fluid motion were not included in the data evaluation. The temperatures measured in the coolant jets' core regions resemble the temperature of the preheated air of 450 K. Within the first 2 mm off the wall, the penetrating air jets form a coolant film, which starts at the lowest jet and is preserved downstream in vertical direction. As the FRS signal depends on the scattering gas species inside the probe volume, the highest accuracy of the FRS measurement is expected within the first two millimetres from the wall, where the coolant film mainly consists of air streaming out of the cooling holes. With increasing distance from the wall, the coolant film starts mixing with the combustor's exhaust gas, making the determination of the gas composition difficult. LIF flame temperatures (compare x = 4 - 5 mm in [Lange2012]) indicate a 150 K higher temperature in this region. This bias was confirmed by evaluating the McKenna burner data from section 4.1 using air instead of exhaust gas. Nevertheless the Rayleigh temperature of the air jets agreed within about 25 K with thermocouple measurements of the preheated air. Finally a spatially resolved 2 D

impression of the cooling film was obtained. Even close to the highly luminescent flame zone (skipped white area within Fig. 10) and in close vicinity to the reflecting cooling wall the flow structures are resolved.

5. Conclusion

A frequency scanning FRS system based on a continuous wave light source was developed and successfully applied in the context of combustion experiments under atmospheric laboratory conditions as well as in a pressurized test rig environment. Regarding measurements in testing facilities, where conditions are harsh and space is confined, the compact (laser head 18 x 14 x 47 cm^3, power supply 27 x 50 x 50 cm^3) and robust Coherent Verdi laser offers superior stability over FRS systems using pulsed light sources. Despite an increased susceptibility to soot luminescence or blackbody radiation due to longer camera exposures, the advantages of the cw-laser based system lie in its narrow linewidth (5 MHz compared to 100 – 150 MHz), independence of undesired line broadening effects (Lorentzian wings or second modes) and an improved signal to noise ratio. The system is aimed at investigating steady phenomena or at obtaining mean values in unsteady flows. By limiting the scanning frequencies to values of high molecular absorbance of the molecular absorption filter, the system becomes independent of strong elastic stray light sources. Thus the system is capable of providing measurements in the direct vicinity of highly illuminated walls. Concerning ambiguity and temperature sensitivity, the frequency scanning method, based on evaluating intensity spectra, promises a reduced uncertainty in comparison to single frequency approaches.

In investigating an atmospheric CH_4/Air flame, the fs-FRS results are in very good agreement to temperature values obtained with CARS. The residual uncertainty of the fs-FRS data fit is well below 1 %. The fs-FRS system offers an accessibility of temperatures ranging from well below room temperature up to temperatures well above 1500 K and thereby complements the established OH-LIF techniques [Heinze2011, Lange2012].

Being optimized with respect to background suppression, temperature sensitivity and mechanical-/ thermal stability the presented fs-FRS system proved its applicability and reliability under test rig conditions. The application example presented herein demonstrates for the first time that high spatial resolution near-wall measurements can be achieved in a generic combustor operating at 5 bar. The temperature values inside the cooling jets' cores obtained with fs-FRS match the thermocouple measurements of the preheated air within 25 K. In the direct vicinity of the liner wall, where OH-LIF is limited by low OH concentrations, fs-FRS was capable to give a 2 D impression of the flow structures of coolant film interacting with the combustor's main flow. The temperature field of Fig 10 was determined neglecting Doppler shifts arising from convective fluid motion. Considering the cooling jets' core regions, where velocities of about 50 m/s are expected, the assumption leads to an increased residuum in the data fit. In a next step of data evaluation, in incorporating the Doppler shift both the residual should be further reduced as well as information on velocity in this region should be gained.

Potential applications of the presented fs-FRS system lie within combustion research as well as in the investigation of non-reacting flows. In this regard, the greatest demands can be found within the field of machine-oriented testing facilities. In an on-going effort to qualify the FRS technique for harsh environments, the system has been implemented on probe-based technology with respect to high power laser light transfer through fibres as well as observation using image fibre bundles [Stockhausen2010].

The first steps into pressurized environments have proved very encouraging regarding future applications at DLR Cologne's high pressure combustion chamber test rig, which is capable to provide working pressures up to 40 bar. The fs-FRS will be applied to characterize the combustor's exhaust gas temperature distribution. In non-reacting flows the fs-FRS will contribute to

characterize the inlet temperature of a high pressure two-stage turbine with simulated combustor flow. The "Next Generation Turbine Test Facility", located at DLR Göttingen, is under construction and will be operational in 2013.
Considering the above mentioned high pressure turbine and combustor applications, optical accessibility will be reduced to a minimum. In machine-oriented test rigs large optical quality windows are both a question of cost as well as operational security. The probe-based realisation of the FRS system guarantees a minimum of invasiveness. Optical probes can be applied to openings already existing for conventional probe-based techniques.

6. Acknowledgements

The authors gratefully acknowledge the good corporation with the Institute of Propulsion Technology's combustion department, namely Dr. Thomas Behrendt in offering the possibility to test the fs-FRS technique on the single sector combustor rig. Concerning the optical design of the camera system, the authors gratefully acknowledge Joachim Klinner. Special thanks go to Manfred Beversdorff who designed the camera system and realised a new iodine filter concept.

7. References

Behrendt T, Lengyel T, Hassa C, Gerendás M (2008) Characterization of advanced combustor cooling concepts under realistic operating conditions. Proceedings of ASME Turbo Expo 2008: Power for Land, Sea and Air, June 9-13, Berlin, Germany, GT2008-51191

Boguszko M, Elliott G (2005) On the use of filtered Rayleigh scattering for measurements in compressible flows and thermal fields. Experiments in Fluids 38 (1): 33-49.

Brübach J, Zetterberg J, Omrane A, Li ZS, Aldén M, Dreizler A (2006) Determination of surface normal temperature gradients using thermographic phospshors and filtered Rayleigh scattering. Appl. Phys. B 84: 537–541.

Elliott GS, Glumac N, Carter CD, Nejad AS (1997) Two-Dimensional Temperature Field Measurements Using a Molecular Filter Based Technique. Combustion Science and Technology 125 (1): 351-369.

Elliott GS, Glumac N, Carter CD (2001) Molecular filtered Rayleigh scattering applied to combustion. Measurement Science and Technology 12 (4): 452.

Forkey J (1996a) Development and Demonstration of Filtered Rayleigh Scattering: a Laser Based Flow Diagnostic for Planar Measurement of Velocity, Temperature and Pressure. PhD thesis, Princeton University.

Forkey J, Finkelstein N, Lempert W, Miles R (1996b) Demonstration and characterization of filtered Rayleigh scattering for planar velocity measurements: Aerodynamic measurement technology, AIAA journal 34 (3): 442-448.

Fourguette D, Zurni, Long M (1986) Two-dimensional Rayleigh thermometry in a turbulent nonpremixed methane-hydrogen flame. Combustion science and technology 44 (5): 307-317.

Gerendás M, Höschler K, Schilling T (2001) Development and Modeling of Angled Effusion Cooling for the BR715 Low Emission Staged Combustor Core Demonstrator. Paper presented at the RTO AVT Symposium on "Advanced Flow Management: Part B – Heat Transfer and Cooling in Propulsion and Power Systems", held in Loen, Norway, 7-11 May, and published in RTO-MP-069(I)

Heinze J, Meier U, Behrendt T, Willert C, Geigle KP, Lammel O, Lückerath R (2011) PLIF Thermometry Based on Measurements of Absolute Concentrations of the OH Radical. Zeitschrift für Physikalische Chemie 225 (11-12): 1315-1341.

Kearney SP, Schefer RW, Beresh SJ, Grasser TW (2005) Temperature imaging in nonpremixed flames by joint filtered Rayleigh and Raman scattering. Applied Optics 44 (9): 1548-1558.

Lange L, et al (2012) Combination of Planar Laser Optical Measurement Techniques for the

Investigation of Pre-mixed Lean Combustion. 16th Int Symp on Applications of Laser Techniques to Fluid Mechanics, Lisbon, Portugal, 09-12 July

Meier U, Heinze J, Freitag S, Hassa C (2011) Spray and Flame Structure of a Generic Injector at Aeroengine Conditions. Proceedings of ASME Turbo Expo, June 6-10, Vancouver, Canada GT2011-45282

Mielke A, Elam K (2009) Dynamic measurement of temperature, velocity, and density in hot jets using Rayleigh scattering. Experiments in fluids 47 (4): 673-688.

Miles RB, Lempert W (1990) Two-dimensional measurement of density, velocity, and temperature in turbulent high-speed air flows by UV rayleigh scattering. Applied Physics B: Lasers and Optics 51: 1-7.

Miles RB, Lempert WR, Forkey JN (2001) Laser Rayleigh scattering. Measurement Science and Technology 12 (5): 33.

Most D, Leipertz A (2001) Simultaneous Two-Dimensional Flow Velocity and Gas Temperature Measurements by use of a Combined Particle Image Velocimetry and Filtered Rayleigh Scattering Technique. Applied Optics 40 (30): 5379-5387.

Panda J, Seaseholtz RG (2004) Velocity and Temperature Measurement in Supersonic Free Jets Using Spectrally Resolved Rayleigh Scattering. Technical report, NASA.

Pitz R, Cattolica R, Robben F, Talbot L (1976) Temperature and density in a hydrogen—air flame from Rayleigh scattering. Combustion and Flame 27: 313-320.

Röhle I, Willert CE (2001) Extension of Doppler global velocimetry to periodic flows. Measurement Science and Technology 12 (4): 420.

Stockhausen G, Doll U, Strehlau T, Willert CE (2010) Combined filtered Rayleigh and Mie scattering for simultaneous planar temperature and velocity measurements. 15th Int Symp on Applications of Laser Techniques to Fluid Mechanics, Lisbon, Portugal, 05-08 July

Sutton G, Levick A, Edwards G, Greenhalgh D (2006) A combustion temperature and species standard for the calibration of laser diagnostic techniques. Combustion and Flame 147 (1-2): 39-48.

Tenti G, Boley C, Desai R (1974) On the Kinetic Model Description of Rayleigh-Brillouin Scattering from Molecular Gases. Canadian Journal of Physics 52 (4): 285-290.

Vetterling W, Flannery B, Press W, Teukolski S (1992) Numerical Recipes in Fortran- The art of scientific computing. Cambridge University Press

Vieitez MO, van Duijn EJ, Ubachs W, Witschas B, Meijer A, de Wijn AS, Dam NJ, van de Water W (2010) Coherent and spontaneous Rayleigh-Brillouin scattering in atomic and molecular gases and gas mixtures, Phys. Rev. A 82, 043836.

Weigand P, Lückerath R, Meier W Documentation of Flat Premixed Laminar CH4/Air Standard Flames: Temperatures and Species Concentrations. www.dlr.de/VT/Datenarchiv

Young AT, Kattawar GW (1983) Rayleigh-scattering line profiles, Applied Optics 22 (23): 3668-3670.

Zetterberg J, Li Z, Afzelius M, Aldén M (2008) Two-Dimensional Temperature Measurements in Flames Using Filtered Rayleigh Scattering at 254 nm. Appl. Spectrosc. 62 (7): 778-783.